Genes & Diseases (2022) 9, 1716–1726

Available online at www.sciencedirect.com

ScienceDirect

journal homepage: http://ees.elsevier.com/gendis/default.asp

FULL LENGTH ARTICLE

Tetratricopeptide repeat domain 36 deficiency mitigates renal tubular injury by inhibiting TGF-β1-induced epithelial–mesenchymal transition in a mouse model of chronic kidney disease

Xin Yan [1], Rui Peng [1], Yilu Ni, Lei Chen, Qingling He, Qianyin Li **, Qin Zhou*

The Ministry of Education Key Laboratory of Clinical Diagnostics, School of Laboratory Medicine, Chongqing Medical University, Chongqing 400016, PR China

Received 8 January 2021; received in revised form 6 April 2021; accepted 20 April 2021
Available online 14 May 2021

KEYWORDS
CCAAT enhancer binding protein beta;
Chronic kidney disease;
Epithelial–mesenchymal transition;
Renal fibrosis;
SMAD family bember 3;
Tetratricopeptide repeat domain 36

Abstract The damage of proximal tubular epithelial cells (PTECs) is considered a central event in the pathogenesis of chronic kidney disease (CKD) and deregulated repair processes of PTECs result in epithelial–mesenchymal transition (EMT), which in turn aggravates tubular injury and kidney fibrosis. In this study, we firstly revealed that the reduction of TTC36 is associated with unilateral ureteral obstruction (UUO)-induced CKD; besides, ablation of TTC36 attenuated tubular injury and subsequent EMT in UUO-treated mice kidneys. Consistently, TTC36 overexpression promoted EMT in TGF-β1-induced HK2 cells. Moreover, TTC36 elevated the protein expression of CEBPB, which was involved in the regulation of TGF-β/SMAD3 signaling, and augmented SMAD3 signaling and downstream genetic response were reduced by CEBPB silencing. Collectively, our results uncovered that TTC36 deficiency plays a protective role in tubular injury and renal fibrosis triggered by UUO; further, TTC36 overexpression exacerbated TGF-β/SMAD3 signaling via elevating the stability of SMAD3 and CEBPB, suggesting that TTC36 inhibition may be a potential strategy in the therapy of obstructive nephropathy.

* Corresponding author.
** Corresponding author.
E-mail addresses: liqianyin904@cqmu.edu.cn (Q. Li), zhouqin@cqmu.edu.cn (Q. Zhou).
Peer review under responsibility of Chongqing Medical University.
[1] Contributed equally to this work.

https://doi.org/10.1016/j.gendis.2021.04.005

Introduction

Chronic kidney disease (CKD), with the characteristic of kidney fibrosis consisting of glomerulosclerosis and tubulointerstitial fibrosis (TIF), is a serious syndrome accompanied by progressively renal function deterioration and potential lethal risk.[1–4] Cellular injury, especially renal proximal tubular epithelial cells (PTECs), initiate CKD and the deregulated repair processes of PTECs results in cellular epithelial–mesenchymal transition (EMT), which in turn exacerbate the progression of CKD and kidney fibrosis.[5–9]

During the EMT process, tubular epithelial cells undergo a series of changes, including differentiation, losing polarity, enhancing migratory capacity, and increasing production of extracellular matrix (ECM) components, along with an upregulation of mesenchymal markers containing vimentin (VIM) and cadherin 2 (CDH2, also known as N-cadherin), and a downregulation of epithelial signatures including tight junction protein 1 (TJP1, also known as ZO-1) and cadherin 1 (CDH1, also known as E-cadherin).[10–12]

Recognized as a potent inducer of EMT, transforming growth factor β1 (TGF-β1) takes effect through binding with the TGF-β type II receptor (TGF-β R II), which phosphorylates the TGF-β RI, leading to the activation of SMAD family member 2/3 (SMAD2/3).[13–15] After activated, the SMAD complex, consisting of SMAD2, SMAD3, and SMAD4, translocate into the nucleus and initiate the process of EMT and up-regulate the expression of profibrotic genes including *ACTA2* (actin alpha 2, smooth muscle, also known as α-SMA), *COL1A1* (collagen type I alpha 1 chain, also known as COL-1), and *SNAI1* (snail family transcriptional repressor 1).[16–20]

SMAD3 is considered as a pivotal transcription factor which is activated in answer to multiple fibrogenic mediators[21]; however, knockout of *SMAD3* contributes to autoimmune disease.[22,23] Currently, no specific therapy is available to mitigate renal fibrogenesis and protect organic function. Therefore, alternative approaches to suppress the TGF-β/SMAD signaling could be of significance in suppressing renal fibrosis without disturbing the immune system.

Tetratricopeptide repeat domain 36 (*TTC36*) is primarily expressed in liver and PTECs, encoding the protein which has three tetratricopeptide repeats and functions as a chaperone for heat shock protein 70. It is reported that TTC36 is downregulated in hepatocellular carcinoma (HCC), serving as a tumor suppressor since it facilitates apoptosis in HCC.[24] In mice models, TTC36 deficiency results in tyrosinemia type III because it enhances the stability of 4-hydroxyphenylpyruvic acid dioxygenase (HPD) catalyzing 4-hydroxy-phenylpyruvic acid into homogentisic acid in liver via preventing TTC36 from STK33 and PELI1-induced degradation.[25] However, no study reveals the role of TTC36 in the pathogenesis of renal fibrosis.

In this study, we investigated the underlying role of TTC36 in the pathogenies of CKD and their potential mechanisms. We identified that TTC36-deficiency attenuated the damage and EMT of PTECs induced by unilateral ureteral obstruction (UUO), whereas TT36 overexpression promoted TGF-β1 mediated EMT and cell cycle arrest, potentially by enhancing the stability of SMAD3 and CCAAT enhancer binding protein β (CEBPB). These findings augmented the understanding of intricate TGF-β/SMAD3 signaling regulation, implying a potential therapeutic approach to renal fibrosis.

Materials and methods

Materials

Rabbit anti-SMAD2/3 (#8685), anti-SMAD3 (#9523), anti-α-SMA (#19245), anti-Phospho-SMAD3 (#9529), anti-SNAI1 (#3879), anti-VIM (#5741), and anti-TWIST1 (#46702) were purchased from Cell Signaling Technology (Danvers, MA, USA). Rabbit anti-N-cadherin (ab18203) was bought from Abcam (Shanghai, China). Mouse anti-Flag (AP0007M) was obtained from Bioworld Technology (St. Louis Park, MN, USA). Mouse anti-β-Tubulin (HC101-01), anti-β-Actin (HC201-01), and anti-GAPDH (HC301-01) were purchased from TransGen Biotech (Beijing, China). Mouse anti-CEBPB (sc-7962) was obtained from Santa Cruz Biotechnology (Santa Cruz, CA, USA). Rabbit anti-TTC36 was manufactured form previous work.[26] Human TGF-β1 protein (10804-HNAC) was bought from SinoBiological (Beijing, China). To process Immunohistochemical (IHC) staining, SP kit (SP-9001) and Diaminobenzidine (DAB) coloring system (ZLI-9017) were purchased from ZSGB-BIO (Beijing, China).

DNA constructs

For the overexpression of TTC36, amplified with PCR, human TTC36 (NM_001080441.4) was subcloned into the CMV vector to construct TTC36 overexpression vector.

Mice and models

Ttc36 knockout (*Ttc36*$^{-/-}$) C57BL/6 mice were obtained from previous work[27] and were fed in the animal center in which food and water were adequately prepared. Compared to wild-type (WT) C57BL/6, they could develop normally, even though they will suffer from tyrosinemia type III when they are 8–12-months old. Eight-week-old male WT C57BL/6 mice were purchased from the Laboratory Animal Centre of Chongqing Medical University (No. SYXK2018-0003, Chongqing, China). A total of 24 mice were employed in this study, including 18 WT and 6 *Ttc36*$^{-/-}$ C57BL/6 mice. To explore the correlation of TTC36 expression with the progression of CKD, 8-week-old male WT C57BL/6 mice were assigned to four groups (Sham, $n = 3$; 3 days after UUO, $n = 3$; 7 days after UUO, $n = 3$; 14 days after UUO, $n = 3$). To study the function of TTC36 in UUO-induced CKD, 8-week-old male WT and *Ttc36*$^{-/-}$ C57BL/6 mice were divided into four groups (WT-sham, $n = 3$; *Ttc36*$^{-/-}$-sham, $n = 3$; WT-UUO, $n = 3$; *Ttc36*$^{-/-}$-UUO, $n = 3$). After 7 days, the mice were anesthetized with diethyl ether, and the kidney and blood were obtained, then the mice were sacrificed with overdose of anesthesia. All animal experiments were processed under the permission of the Animal Ethical

Commission of Chongqing Medical University. In brief, after anesthetized with diethyl ether, the mice (male, aged 8—10 weeks) were warmed at 37.0°C and were subjected to UUO by ligating the left ureter with sutures. As a control group (Sham), the left ureters of mice were exposed, without ligation. After surgery, mice were looked after carefully and sacrificed at specific time to obtain kidneys for mRNA quantification, Western blotting, Hematoxylin-Eosin (H&E) staining, and immunohistochemical (IHC) staining. The concentration of blood urea nitrogen (BUN) and serum creatinine (SCr) were detected with BUN Detection Kit and SCr Detection Kit (Nanjing Jiancheng Bioengineering Institute) respectively.

Cell culture, lentivirus infection and treatment

The human proximal tubular epithelial cells (HK2) were maintained in the medium consisting of Dulbecco's modified Eagle's medium-F12 (DMEM/F12, Gibco), 10% fetal bovine serum (FBS, Biological Industries), and 1% penicillin-streptomycin (HyClone). For the package of lentivirus, HEK293T cells were cultured in DMEM medium (Gibco) supplemented with 10% FBS (Biological Industries) and 1% penicillin-streptomycin (HyClone) and were transfected with TTC36 overexpression constructs and lentivirus backbone vectors using TurboFect™ Transfection Reagent (Thermo Scientific) according to the manual. To concentrate lentivirus, the transfected cells and supernatant were collected and centrifugated at the speed of 25,000×*g* for 2 h at 4°C. HK2 cells were infected by lentivirus in the presence of 8 μg/ml polybrene (Sigma). For the selection of stable clones, HK2 cells were treated with puromycin (Invitrogen). To silence the expression of TTC36 (or CEBPB), si-RNA (si-TTC36, sequence 5′-GGAAGAACGAGAAGAA-GAUGA-3'; si-CEBPB, 5′-GGUGUUAUUUAAAGAAGAA-3′) were obtained from GenePharma (Shanghai, China), and were transfected into HK2 cells with Lipofectamine 2000 Transfection Reagent (Invitrogen) according to the guidance of manufacture. To induce EMT, HK2 cells were incubated with 10 ng/ml TGF-β1 for 48 h.

H&E staining and IHC staining

For H&E staining, after harvested, mouse kidneys were fixed in 4% formaldehyde, embedded in paraffin, and cut into 4 μm sections. The sections were dewaxed with xylene and rehydrated by ethyl alcohol solution with series concentration, stained with hematoxylin for 2 min, washed with water for 2 min, destained with acid alcohol for 2 s, rinsed with water for 2 min, soaked in lithium carbonate for 2 min, flushed with water for 2 min, soaked in 80% ethanol for 1 min, and counterstained with eosin for 1 min. To perform histological evaluation and scoring, the parameters of tubular dilation, border loss, cast deposition, border necrosis, and tuft adhesion or sclerosis in sections were counted and scored under 200× magnification and were used to value the degree of proximal tubular pathological injury and functional changes.[28]

To process IHC staining, after dewaxed and rehydrated as above description, the sections were heated at 100 °C for 20 min in Tris buffer (pH = 9.0) to antigen retrieving, treated with hydrogen-peroxide-solution for 10 min to eliminate endogenous peroxidase, coated with goat serum for 30 min to block nonspecific antigen, incubated with primary antibody at 4°C overnight, washed with phosphate buffer saline containing 0.05% Tween20 (PBST), treated with biotin labeled secondary antibody for 15 min, and coated with horseradish peroxidase conjugated with streptavidin for 15 min. Finally, the sections were stained with DAB coloring system under the guidance of manufacture. The IHC scoring was performed using Image-Pro Plus 6.0 software (Media Cybernetics, MD, USA).

Western blotting analysis

After rinsed three times with cold PBS, cells were lysed using lysis buffer (50 mM Tris—HCl pH 7.5, 1 mM EDTA, 150 mM NaCl, 2 mM Vanadate, 1 mM PMSF, protease inhibitor (APExBIO), Phosphatase Inhibitor (APExBIO), and 1% SDS), and then the protein extraction were transferred to 1.5 ml microtubes and heated at 100 °C for 10 min. After that, the protein extraction was centrifuged at the speed of 10,000×*g* for 10 min and the concentration of protein were quantified with BCA Protein Assay Kit (Thermo Scientific). The equal quantity protein was separated by sodium dodecyl sulfate polyacrylamide gel (SDS-PAGE) and transferred to polyvinylidene difluoride (PVDF) membranes (Millipore). After transferred, the membranes were blocked by 5% fat-free milk (Sangon Biotech) dissolved in Tris-buffered saline (TBS) containing 0.08% Tween 20 (Sigma) at room temperature for 2 h, incubated with primary antibodies at 4°C overnight, washed with TBST, incubated with suitable HRP-conjugated secondary antibodies for 1 h at room temperature, and rinsed with TBST again. The bands were measured using Smart-ECL basic kits (Smart-Lifesciences) and Image Lab software program (Bio-Rad). β-Actin, β-tubulin and GAPDH were used as the loading control. To analyze the integral optical density of target bands, the bands were processed and detected by Image J software.

Immunoprecipitation

Proteins were extracted from HK2 cells with a lysis buffer (50 mM Tris—HCl pH 7.5, 10 mM NaF, 0.1% deoxycholate, 10 mM β-glycerophosphate, 1% NP-40, 1 mM Vanadate, 1 mM PMSF, protease inhibitor, and Phosphatase Inhibitor) and were centrifuged at a speed of 12,000×*g* for 20 min. The supernatants were quantified by BCA Protein Assay Kit (Thermo Scientific) and approximately 1.2 mg protein were subjected to immunoprecipitation with ANTI-FLAG M2 antibody (Sigma—Aldrich). The mixture was incubated at 4 °C overnight, then the protein A/G agarose beads (Smart-Lifesciences) were added. The mixture was incubated at 4 °C for additional 4 h. After that, the immunocomplexes were centrifugated and washed with the lysis buffer for four times. Finally, these immunocomplexes were subjected to Western blotting analysis.

Cell cycle assay

For the detection of cell cycle, after treated, cells were fixed with 75% alcohol at 4 °C overnight, stained with

Propidium (PI), and detected by the flow cytometry platform of Institute of Life Science of Chongqing Medical University using a CytoFLEX flow cytometry (BECKMAN COULTER).

Cell viability assay

HK2 cells were distributed to 96-well plates with 2×10^3 cells per well and were treated with 10 ng/ml TGF-β1 for 24 h, 48 h and 72 h respectively. The cell viability was detected by using Cell Counting Kit-8 (MedChem Express) according to the manual.

Quantitative real-time polymerase chain reaction (RT-qPCR)

To detect the mRNA expression of specific genes in cells and kidneys, cells or kidneys were lysed using TRIzol reagent

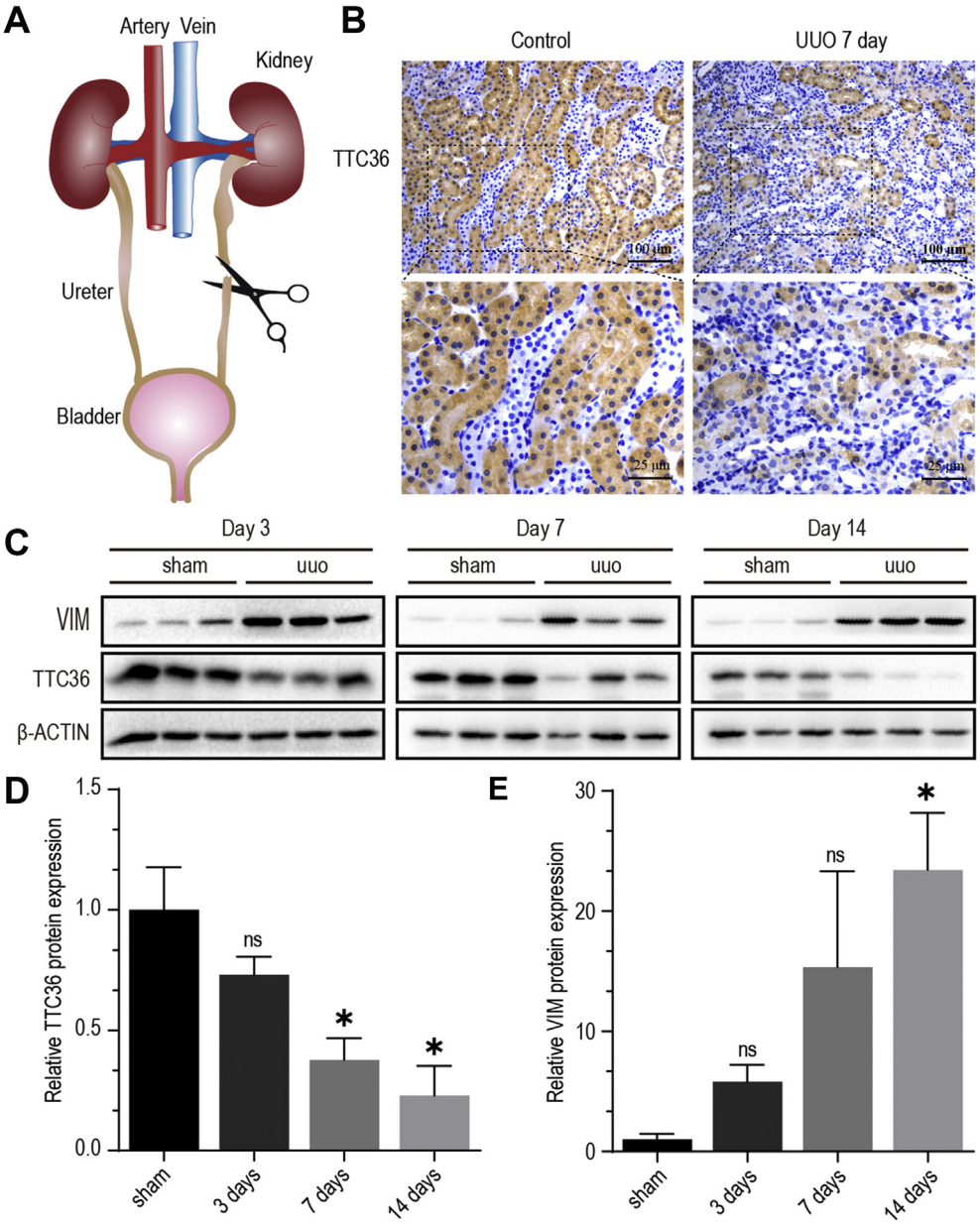

Figure 1 The reduction of TTC36 in kidneys was associated with CKD. **(A)** Surgery strategy of UUO to induce CKD. **(B)** Representative images of IHC staining for TTC36 in kidney sections from UUO-induced WT mice for 7 days, Sham group as a control ($n = 3$; upper images scale bars, 100 μm; lower images scale bars, 25 μm). **(C)** Western blotting for TTC36 and VIM in the kidneys of mice with UUO-induced CKD (3, 7 and 14 days after UUO-treatment; $n = 3$ per group); β-ACTIN was used as a loading control. **(D)** Quantitative analysis for the expression of TTC36 relate to β-ACTIN by detecting integral optical density for (C). **(E)** Quantitative analysis for the expression of VIM relate to β-ACTIN using the detection of integral optical density for (C). Data are shown as means ± SD. Statistically significant differences were calculated by Student's *t*-test and ANOVA. $^*P < 0.05$ versus sham group. Results are representative of three independent experiments. UUO, unilateral ureteral obstruction; CKD, chronic kidney disease; TTC36, tetratricopeptide repeat domain 36; VIM, Vimentin; SD, standard deviation; ANOVA, one-way analysis of variance.

(Invitrogen). The total RNA was extracted with chloroform, precipitated by isopropanol, washed with 75% ethyl alcohol twice, and dissolved by DNase/RNase-free water (Solarbio). The total RNA was reversely transcript to cDNA using RevertAid RT Reverse Transcription Kit (Thermo Scientific) according to manual. Then, the cDNA library was amplified using specific primers of genes and 2 x SYBR Green qPCR Master Mix (bimake) under a CFX96 real-time PCR detection system (Bio-Rad). The relative expression level of genes was calculated relative to the mean critical threshold (CT) values of the 18S gene. Specific primers sequences of genes were listed in Table S1.

Statistical analyses

All experiments were independently performed three times to confirm the results. Data were shown as mean ± standard deviation with GraphPad Prism 8 software, and the statistically significant differences were analyzed using analysis of variance (ANOVA), followed by a Student's *t*-test with IBM SPSS Statistics 20 software. Differences were considered as significant with $P < 0.05$. $^{*}P < 0.05$, $^{**}P < 0.01$, and $^{***}P < 0.001$.

Results

The reduction of TTC36 in kidneys was associated with CKD

First, we established the mice model of CKD with the strategy of UUO, as shown in Figure 1A. Next, a distinct reduction of TTC36 expression was observed in kidneys from UUO-treated mice in a time-depend manner, compared to sham group (Fig. 1B—D). The expression of VIM, a mesenchymal marker, was up-regulated over time after UUO-treatment (Fig. 1C, E), confirming the involvement of EMT in the progression of CKD. These data suggested that the down-regulated TTC36 is related to the pathogenesis of CKD.

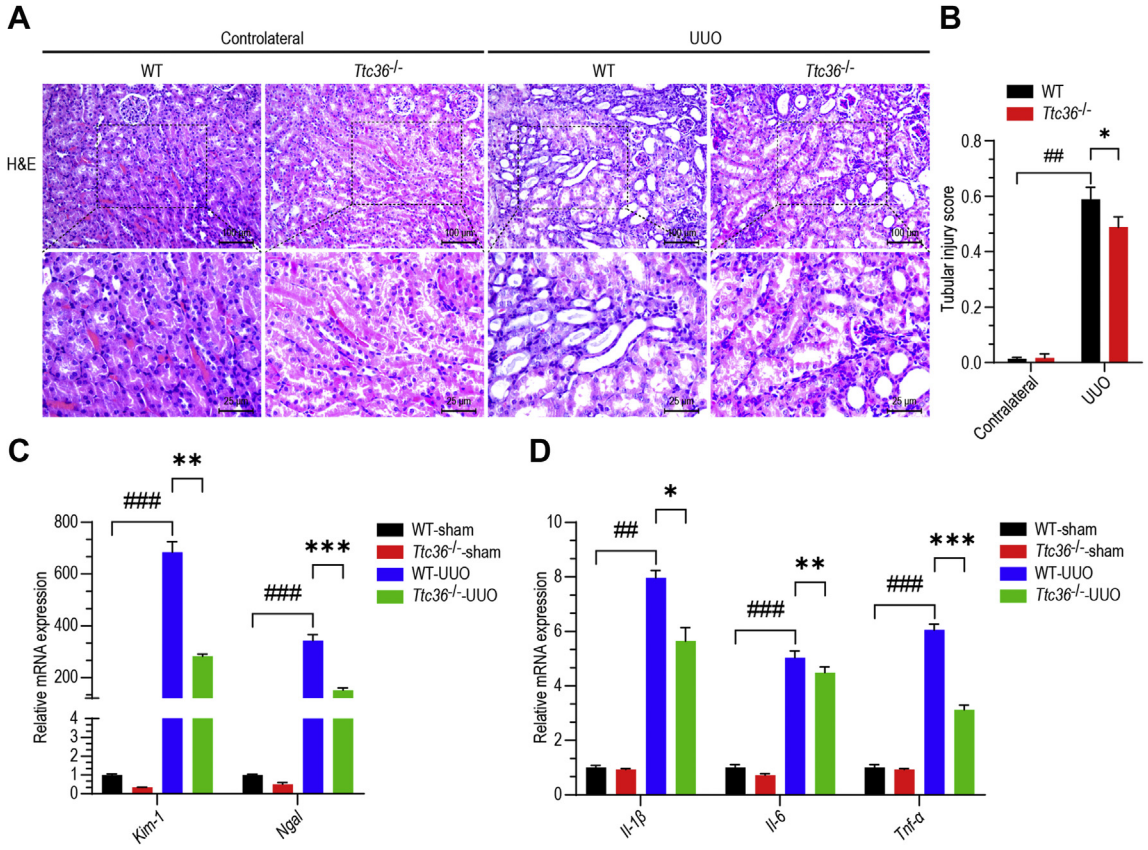

Figure 2 The absence of TTC36 mitigated UUO-mediated PTECs injury and inflammation. **(A)** Representative images of H&E staining in the kidneys of mice treated with UUO for 7 days, contralateral kidney as control ($n = 3$; upper images scale bars, 100 μm; lower images scale bars, 25 μm). **(B)** Tubular injury scores in mice were calculated. At least six random fields were taken from each kidney. **(C)** RT-qPCR analysis for *Kim-1* and *Ngal* mRNA expression in the kidney of UUO-induced mice (WT-sham, *Ttc36*$^{-/-}$-sham, WT-UUO, and *Ttc36*$^{-/-}$-UUO; $n = 3$); 18s was used as an internal control. **(D)** RT-qPCR analysis for *Il-1β*, *Il-6*, and *Tnf-α* mRNA expression in the kidney of UUO-induced mice (WT-sham, *Ttc36*$^{-/-}$-sham, WT-UUO, and *Ttc36*$^{-/-}$-UUO; $n = 3$); 18s was used for an internal control. Data are shown as means ± SD. Statistically significant differences were determined by Student's *t*-test and one-way ANOVA. $\#\#P < 0.01$, and $\#\#\#P < 0.001$ versus WT-sham group; $^{*}P < 0.05$, $^{**}P < 0.01$, and $^{***}P < 0.001$ versus WT-UUO group. Results are representative of three independent experiments. H&E, hematoxylin-eosin; UUO, unilateral ureteral obstruction; RT-qPCR, quantitative real-time polymerase chain reaction; *Kim-1*, kidney injury molecule 1; *Ngal*, neutrophil gelatinase-associated lipocalin; *Il-1β*, interleukin-1β; *Il-6*, interleukin-6; *Tnf-α*, tumor necrosis factor; SD, standard deviation; ANOVA, one-way analysis of variance.

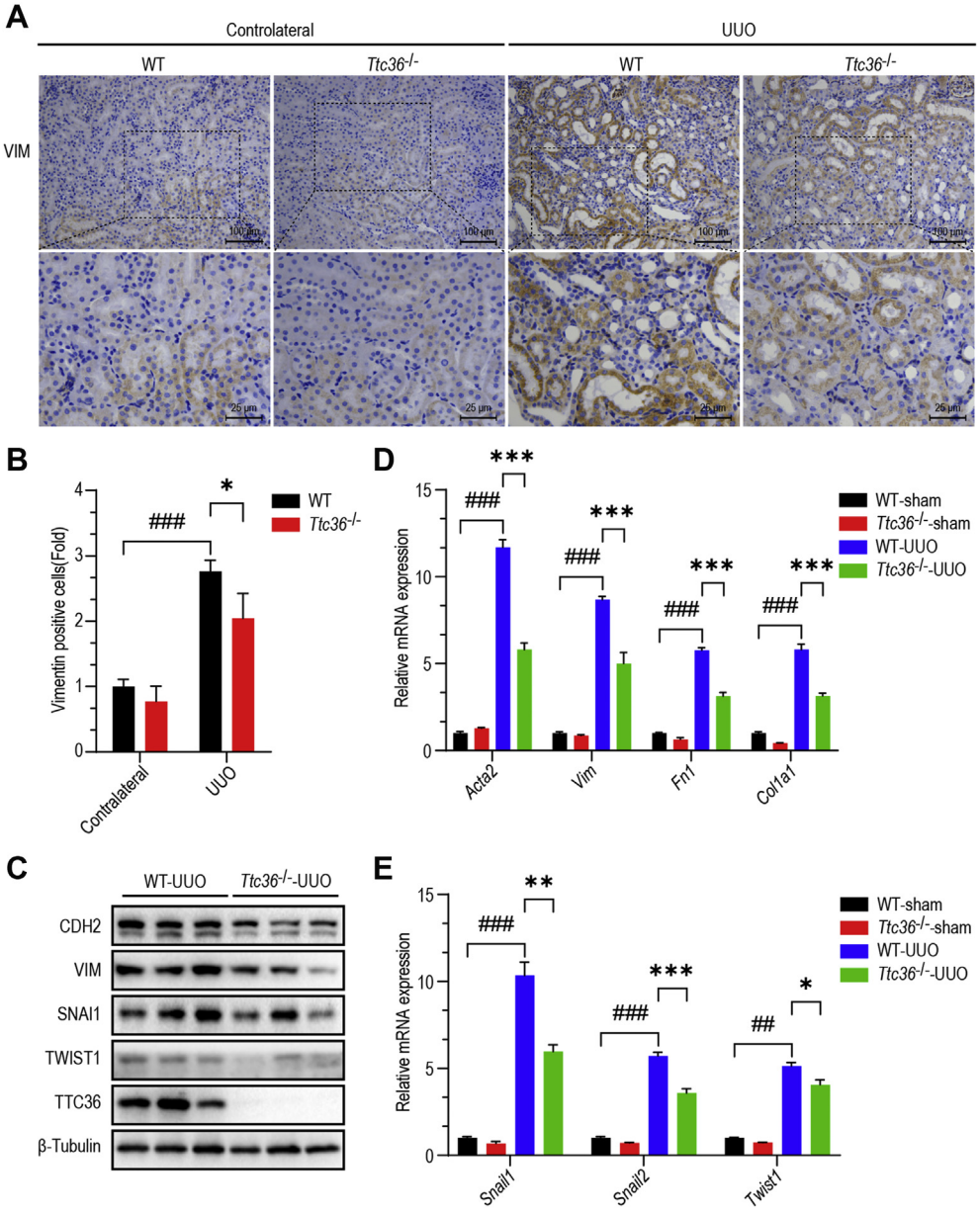

Figure 3 TTC36 depletion ameliorated UUO-induced EMT and renal fibrosis. **(A)** Representative images of IHC staining for VIM in kidney sections from UUO-induced mice for 7 days, contralateral kidney as control ($n = 3$; upper images scale bars, 100 μm; lower images scale bars, 25 μm). **(B)** IHC scores in mice were analyzed. At least eight random fields were taken from each kidney. **(C)** Western blotting for CDH2, VIM, SNAI1, TWIST1, and TTC36 in the kidneys of mice with UUO-induced CKD (WT-UUO and *Ttc36*$^{-/-}$-UUO; $n = 3$); β-Tubulin as a loading control. **(D)** The mRNA expression of *Acta2*, *Vim*, *Fn1*, and *Col1a1* were detected by RT-qPCR (WT-sham, *Ttc36*$^{-/-}$-sham, WT-UUO, and *Ttc36*$^{-/-}$-UUO; $n = 3$); 18s was used as an internal control. **(E)** The mRNA expression of *Snai1*, *Sani2*, and *Twist1* were detected by RT-qPCR (WT-sham, *Ttc36*$^{-/-}$-sham, WT-UUO, and *Ttc36*$^{-/-}$-UUO; $n = 3$); 18s was used as an internal control. Data are shown as means ± SD. Statistically significant differences were analyzed by Student's *t*-test and one-way ANOVA. ##$P < 0.01$ and ###$P < 0.001$ versus WT-contralateral group or WT-sham group; *$P < 0.05$, **$P < 0.01$, and ***$P < 0.001$ versus WT-UUO group. Results are representative of three independent experiments. IHC, immunohistochemical; VIM, Vimentin; CDH, cadherin 2; UUO, unilateral ureteral obstruction; CKD, chronic kidney disease; *Fn1*, fibronectin 1; *Acta2*, actin alpha 2 smooth muscle; *Col1a1*, collagen type I alpha 1 chain; RT-qPCR, quantitative real-time polymerase chain reaction; SD, standard deviation; ANOVA, one-way analysis of variance.

The absence of TTC36 mitigated UUO-mediated PTECs injury and inflammation

To explore the role of TTC36 in CKD, *Ttc36*-deficient (*Ttc36*$^{-/-}$) mice were subjected to UUO. Although there was no significant difference in the level of BUN and SCr between WT groups and *Ttc36*$^{-/-}$ groups (Fig. S1A, B), however, as shown in Figure 2A and B, that TTC36 deficiency attenuated UUO-induced tubular injury was detected in histological analysis, in comparison to UUO-

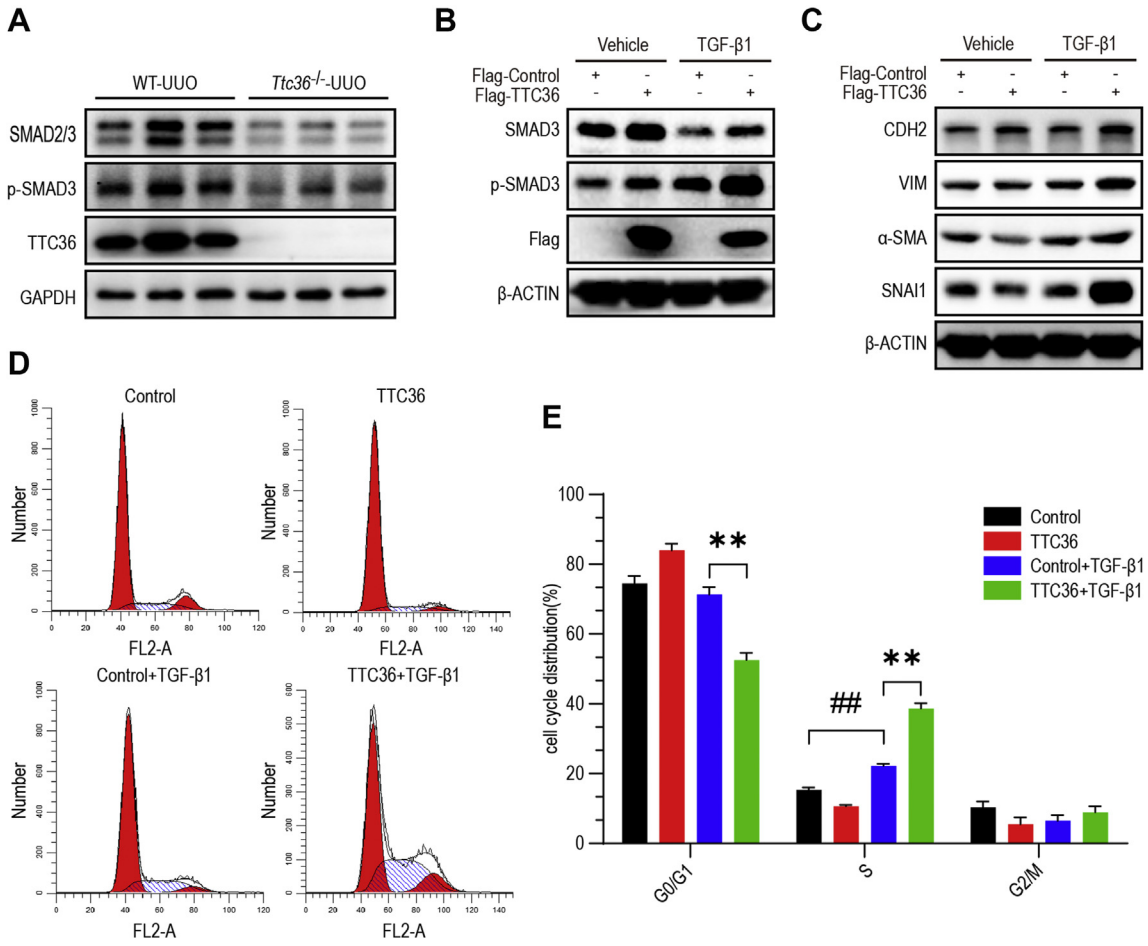

Figure 4 TTC36 overexpression promoted TGF-β/SMAD3 signaling and TGF-β1-induced EMT and cell cycle arrest. **(A)** Western blotting for SMAD2/3, p-SMAD3, and TTC36 in the kidneys of mice treated with UUO for 7 days; GAPDH as a loading control (WT-UUO and *Ttc36*$^{-/-}$-UUO; $n = 3$). **(B)** Western blotting for SMAD3, p-SMAD3, and Flag in TGF-β1-induced HK2 cells for 48 h with or without TTC36 overexpression; β-Actin was used as a loading control. **(C)** Western blotting for CDH2, VIM, ACTA2, and SNAI1 in TGF-β1-induced HK2 cells with or without TTC36 overexpression; β-ACTIN was used as a loading control. **(D)** Representative images for flow cytometry analysis. TTC36 was overexpressed in HK2 cells followed by TGF-β1-treatment for 48 h. **(E)** The percentage of cells in the G0/G1, S, and G2/M phases of the cell cycle are shown. Data are shown as means ± SD. Statistically significant differences were analyzed by Student's *t*-test and one-way ANOVA. ##$P < 0.01$ versus Control group without TGF-β1-treatment; **$P < 0.01$ versus TGF-β1-induced control group. Results are representative of three independent experiments. p-SMAD3, phosphorylated SMAD3; CDH2, cadherin 2; UUO, unilateral ureteral obstruction; ACTA2, actin alpha 2, smooth muscle; GAPDH, glyceraldehyde-phosphate dehydrogenase; TGF-β1, transforming growth factor β1; HK2, human proximal tubular epithelial cell; SD, standard deviation; ANOVA, one-way analysis of variance.

treated WT group. Moreover, we found that the mRNA expression of tubular injury markers (*Kim-1* and *Ngal*) and inflammatory factors (*Il-1β*, *Il-6*, and *Tnf-α*) in the kidneys of UUO-treated *Ttc36*$^{-/-}$ mice were reduced in quantitative real-time polymerase chain reaction (RT-qPCR), compared to WT group treated by the same way (Fig. 2C, D). Collectively, these results demonstrated that TTC36 deficiency protected against renal tubular injury induced by UUO.

TTC36 depletion ameliorated UUO-induced EMT and renal fibrosis

Caused by deregulated repair processes, EMT is recognized as a factor that is responsible for pathological renal fibrosis.[6] To further identify the function of TTC36 involved in UUO-mediated EMT and renal fibrosis, we detected the expression of mesenchymal and profibrotic markers. As shown in Figure 3A and B, the expression of VIM was up-regulated in UUO-treated kidney compared to contralateral kidney and was obviously reduced in the kidney of *Ttc36*$^{-/-}$ mice, in comparison to WT group. Moreover, Western blotting results show that the expression of mesenchymal markers (CDH2 and VIM) and EMT key regulators (SNAI1 and TWIST1) were decreased in *Ttc36*-deficient mice, compared to WT group (Fig. 3C). Consistent with these results, TTC36 depletion lowered the mRNA expression of mesenchymal markers (*Vim* and fibronectin 1 (*Fn1*)), profibrotic genes (*Acta2* and *Col1a1*), and EMT regulators (*Snai1*, *Snai2*, and *Twist1* (twist family

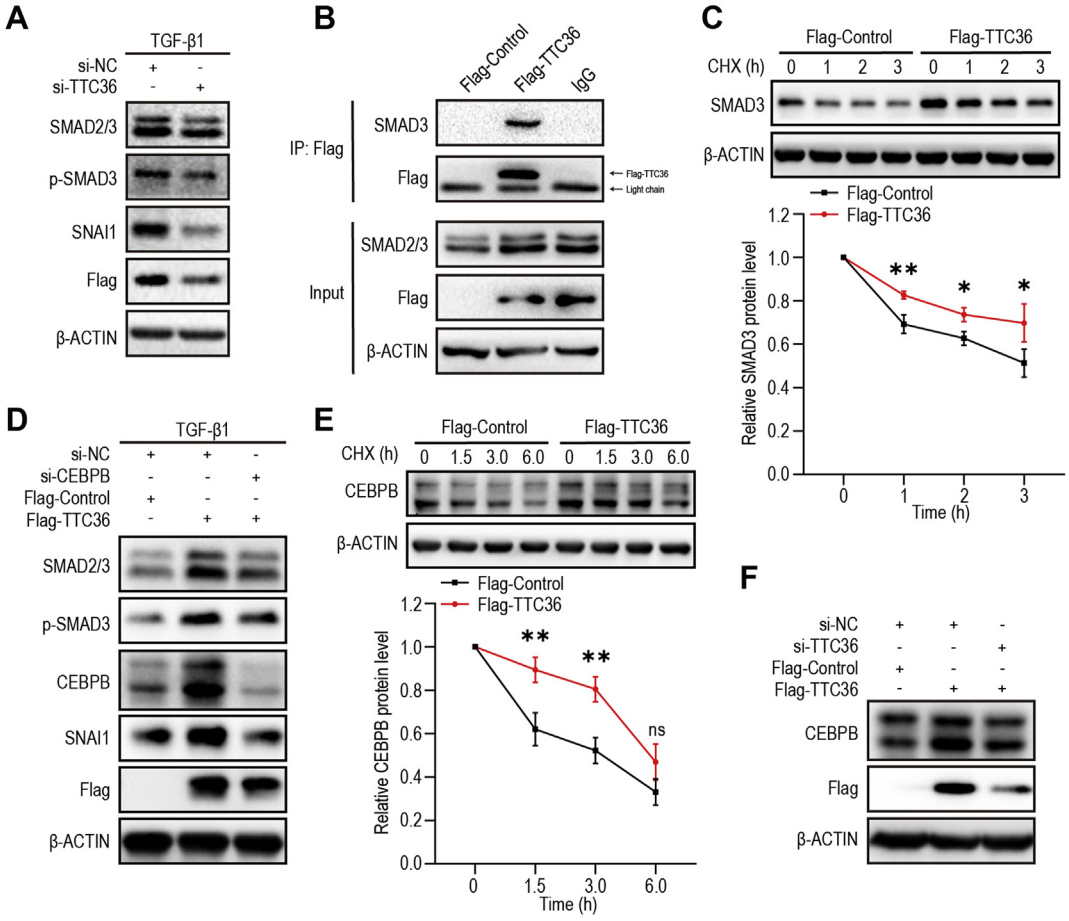

Figure 5 TTC36 promoted TGF-β/SMAD3 signaling via SMAD3 and CEBPB. **(A)** Western blotting for SMAD2/3, p-SMAD3, SNAI1, and Flag in TGF-β1-induced HK2 cells with or without TTC36 silenced; β-ACTIN was used as a loading control. **(B)** Proteins were extracted from HK2 cells and immunoprecipitation for Flag-marked TTC36 was performed with an anti-Flag antibody. Western blotting was performed by using the indicated antibodies. **(C)** HK2 cells expressing Flag-control or Flag-TTC36 were treated with 5 μg/ml cycloheximide for 0, 1, 2, or 3 h; Western blotting for SMAD3; β-ACTIN as a loading control (up); quantification of SMAD3 levels (relative to 0 h, below). **(D)** Western blotting for SMAD2/3, p-SMAD3, CEBPB, SNAI1, and Flag in TGF-β1-treated HK2 cells with or without CEBPB silenced; β-ACTIN was used as a loading control. **(E)** HK2 cells expressing Flag-control or Flag-TTC36 were treated with 5 μg/ml cycloheximide for 0, 1.5, 3, or 6 h; Western blotting for CEBPB; β-ACTIN as a loading control (up); quantification of CEBPB levels (relative to 0 h, below). **(F)** Western blotting for CEBPB and Flag in HK2 cells with or without TTC36 silence; β-ACTIN was used as a loading control. Data are exhibited as means ± SD. Statistically significant differences were analyzed by Student's *t*-test. $^{*}P < 0.05$ and $^{**}P < 0.01$ versus control group. Results are representative of three independent experiments. p-SMAD3, phosphorylated SMAD3; CEBPB, CCAAT enhancer binding protein β; TGF-β1, transforming growth factor β1; HK2, human proximal tubular epithelial cell; SD, standard deviation; CHX, cycloheximide.

bHLH transcription factor 1)) in the kidneys as compared to WT group (Fig. 3D, E). Taken together, these results revealed that TTC36 deficiency attenuated EMT and fibrosis induced by UUO.

TTC36 overexpression promoted TGF-β/SMAD3 signaling and TGF-β1-induced EMT and cell cycle arrest

It is well established that the canonical pathway of TGF-β signaling plays a significant role in EMT.[18] We discovered that the phosphorylated-SMAD3, which is a key transducer of TGF-β signaling and regulates the transcription of EMT related genes,[23] was down-regulated in the kidney of *Ttc36*$^{-/-}$ mice treated by UUO, compared to WT group (Fig. 4A). To further confirm the role of TTC36 in EMT, we employed an *in vitro* EMT model using human proximal tubular cells (HK2) induced by TGF-β1. Consistent with the data *in vivo*, TTC36 overexpression elevated phosphorylated-SMAD3 and upregulated the expression of mesenchymal markers (CDH2 and VIM) and profibrotic genes (*Snai1* and *Acta2*) as compared to TGF-β1-treated control group. Moreover, the TGF-β1-mediated cell cycle arrest was aggravated by TTC36 overexpression, in comparison to control group (Fig. 4D, E). The results of cell viability assay also suggested that TTC36 overexpression significantly enhanced the inhibition of proliferation induced by TGF-β1 (Fig. S2).

Collectively, these results demonstrated that TTC36 overexpression exacerbated TGF-β1-induced EMT and cell cycle arrest by promoting TGF-β/SMAD3 signaling.

TTC36 promoted TGF-β/SMAD3 signaling via SMAD3 and CEBPB

To further confirm the role of TTC36 in TGF-β/SMAD3 signaling pathway, we employed small interfering RNA (si-RNA) to silence TTC36 expression, and observed that, after TTC36 silenced, both the expression and phosphorylation of SMAD3 were reduced, followed by the reduction of SNAI1 in TGF-β1-treated HK2 cells (Fig. 5A). Moreover, the interaction between TTC36 and SMAD3 was observed by immunoprecipitation (Fig. 5B) and the role of TTC36 in elevating the stability of SMAD3 was detected (Fig. 5C). We also detected that TTC36 overexpression up-regulated the mRNA level of *SMAD3* in HK2 cells (Fig. S3). It is reported that CEBPB is involved in the regulation of EMT and TGF-β/SMAD signaling.[29] Therefore, we investigated the expression of CEBPB and discovered that CEBPB expression was increased in TTC36 overexpression HK2 cells and was reduced following TTC36 silence (Fig. 5F). The up-regulated expression and phosphorylation of SMAD3 in TTC36 overexpressed HK2 cells was reduced by CEBPB silence, correspondingly, the expression of SNAI1 was also decreased (Fig. 5D). Furthermore, we observed that the stability of CEBPB was enhanced under the condition of TTC36 overexpression (Fig. 5E). These results implied that TTC36 promoted TGF-β/SMAD3 signaling possibly through SMAD3 and CEBPB collectively. In conclusion, these results revealed that TTC36 plays a promotive role in UUO-triggered tubular injury and TGF-β1-induced EMT via SMAD3 and CEBPB, which is summarized in Figure 6.

Discussion

EMT of PTECs and renal fibrosis has been well established in both TGF-β1-treated cells and animal models.[30–32] In this study, we first revealed that TTC36 exacerbated TGF-β1-induced EMT in HK2 cells and aggravated EMT and tubular injury following UUO-treatment *in vivo*. In both of these models, the expression of EMT and profibrotic markers is reduced in the absence of TTC36, which protected against PTECs injury and attenuated the progression of renal fibrosis.

TGF-β1 plays a dominant role in the initiation and progression of EMT and renal fibrosis, however, its effector SMAD proteins exert different and even adverse functions in the regulation of EMT and fibrosis. One of significant difference between the SMAD proteins is that SMAD3 deficiency decreases collagen deposition in the kidney of UUO-treated mice, compared to WT group[33]; however, a protective antifibrotic role for SMAD2 is identified in conditional gene deletion studies.[34] Here we discovered that the SMAD3 protein level was decreased undergoing TGF-β1 activation (Fig. 4B), which consistent with others' studies,[35] and TTC36 enhanced the phosphorylated SMAD3 induced by TGF-β1, which plays an accelerative role in renal fibrosis triggered by EMT.

It is known that CEBPB, as an important transcription factor, controls the promoter of genes involved in immune and inflammatory responses,[36,37] and is responsible for the TGF-β1-induced cytostatic gene activity.[29] Consistently, we detected that TTC36 up-regulated the protein expression of CEBPB and the augmented TGF-β/SMAD3 signaling in TTC36 overexpressed HK2 cells was rescued by CEBPB silence, suggesting that TTC36 potentially promote CEBPB stability to enhance TGF-β1 activated SMAD3 signaling. However, it still needs more efforts to reveal the detailed mechanism of TTC36 involved in CEBPB regulation.

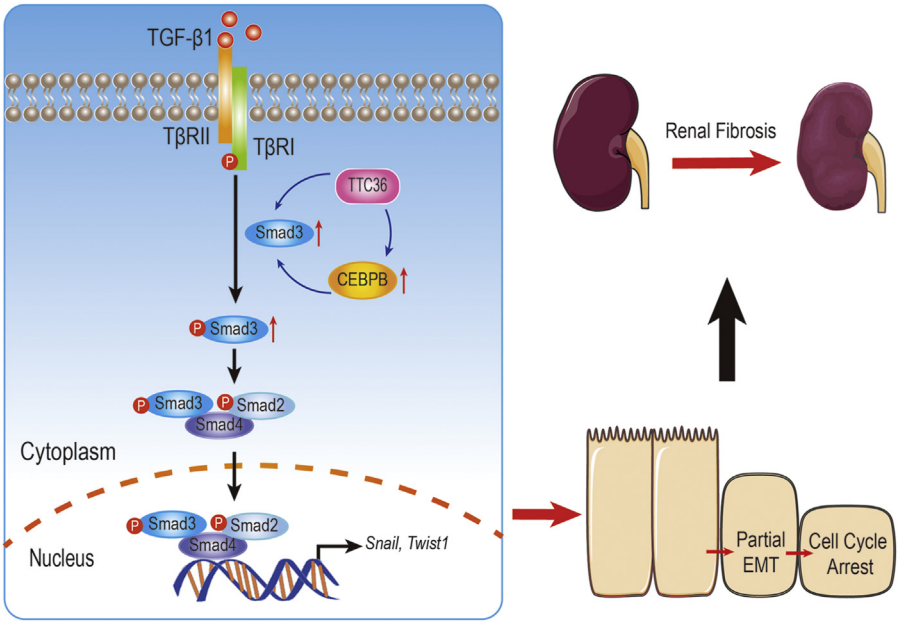

Figure 6 Schematic for TTC6 exacerbating TGF-β1-induced EMT via SMAD3 and CEBPB, exacerbating tubular injury in the mouse model of CKD.

As a strong repressor of E-cadherin gene's transcription, SNAI1 is recognized as an immediate-early gene target of the TGF-β1/SMAD3 pathway and involved in both physiological and pathological EMT.[38–41] In this study, we observed that TTC36 reduced the expression of SNAI1 and ACTA2 in cultured HK2 cells without TGF-β1 treatment (Fig. 4C), suggesting an oppositive role of TTC36 in the regulation of EMT which remains further investigations. However, we did reveal that TTC36 exacerbated TGF-β1-induced EMT and cell cycle arrest, which implied that TTC36 inhibition could attenuate TGF-β1 driven EMT and the expression of profibrotic genes resulted from UUO.

The limitations of our work were that the functions of TTC36 in CKD and renal fibrosis aggravation were mainly observed in mouse and cell models, and lacked of human tissues which may yield more convincing evidence. Moreover, these models used to identify the role of TTC36 in EMT and fibrosis did not directly and completely reflect the complicated human diseases which result in fibrogenesis in the kidney. We did detect the downregulation of TTC36 in the progression of CKD and the promotive effect of TTC36 in EMT induced by TGF-β1. However, the usefulness and significance of TTC36 inhibition in the treatment of CKD patients still need further investigations including patients' specimens plus clinical trials of TTC36 inhibitor in the future.

In conclusion, we demonstrated for the first time that TTC36 deficiency attenuated UUO-induced tubular injury and EMT, whereas TTC36 overexpression exacerbated TGF-β1-mediated EMT and cell cycle arrest, potentially through enhancing the stability of CEBPB and SMAD3. With respect to the more detailed mechanism between TTC36 and CEBPB, further investigation is needed to reveal how TTC36 promotes the stability of CEBPB and whether TTC36 inhibition is a viable therapeutic approach for CKD therapy.

Author contributions

Xin Yan: Conceptualization, Data curation, Formal analysis, Visualization, Roles/Writing – original draft; **Rui Peng:** Investigation, Visualization, Roles/Writing – original draft; **Yilu Ni:** Formal analysis, Visualization; **Qingling He:** Methodology, Writing – review & editing; **Lei Chen:** Software, Writing – review & editing; **Qianying Li:** Funding acquisition, Project administration, Resources, Supervision, Validation; **Qin Zhou:** Funding acquisition, Project administration, Supervision. All authors have read and agreed to the published version of the manuscript.

Conflict of interests

The authors declare no conflict of interest.

Funding

This work was supported by the National Natural Science Foundation of China (No. 81873932, 81802549), the Scientific and Technological Research Program of Chongqing Municipal Education Commission (No. KJQN202000438) and Chongqing Science and Technology Commission (No. cstc2019jscx-dxwtBX0032).

Appendix A. Supplementary data

Supplementary data to this article can be found online at https://doi.org/10.1016/j.gendis.2021.04.005.

References

1. Liu Y. Cellular and molecular mechanisms of renal fibrosis. *Nat Rev Nephrol*. 2011;7(12):684–696.
2. Eddy AA, Neilson EG. Chronic kidney disease progression. *J Am Soc Nephrol*. 2006;17(11):2964–2966.
3. Eddy AA. Overview of the cellular and molecular basis of kidney fibrosis. *Kidney Int Suppl*. 2014;4(1):2–8.
4. Levey AS, Coresh J. Chronic kidney disease. *Lancet*. 2012;379(9811):165–180.
5. Fernandez IE, Eickelberg O. The impact of TGF-β on lung fibrosis: from targeting to biomarkers. *Proc Am Thorac Soc*. 2012;9(3):111–116.
6. Meng XM, Nikolic-Paterson DJ, Lan HY. TGF-β: the master regulator of fibrosis. *Nat Rev Nephrol*. 2016;12(6):325–338.
7. Humphreys BD. Mechanisms of renal fibrosis. *Annu Rev Physiol*. 2018;80:309–326.
8. Ovadya Y, Krizhanovsky V. A new Twist in kidney fibrosis. *Nat Med*. 2015;21(9):975–977.
9. Lovisa S, LeBleu VS, Tampe B, et al. Epithelial-to-mesenchymal transition induces cell cycle arrest and parenchymal damage in renal fibrosis. *Nat Med*. 2015;21(9):998–1009.
10. Kang Y, Massagué J. Epithelial-mesenchymal transitions: twist in development and metastasis. *Cell*. 2004;118(3):277–279.
11. Nieto MA, Huang RY, Jackson RA, Thiery JP. EMT: 2016. *Cell*. 2016;166(1):21–45.
12. Lamouille S, Xu J, Derynck R. Molecular mechanisms of epithelial-mesenchymal transition. *Nat Rev Mol Cell Biol*. 2014;15(3):178–196.
13. Heldin CH, Miyazono K, ten Dijke P. TGF-beta signalling from cell membrane to nucleus through SMAD proteins. *Nature*. 1997;390(6659):465–471.
14. Massagué J. TGF-beta signal transduction. *Annu Rev Biochem*. 1998;67:753–791.
15. Derynck R, Budi EH. Specificity, versatility, and control of TGF-β family signaling. *Sci Signal*. 2019;12(570):eaav5183.
16. Runyan CE, Schnaper HW, Poncelet AC. The phosphatidylinositol 3-kinase/Akt pathway enhances Smad3-stimulated mesangial cell collagen I expression in response to transforming growth factor-beta1. *J Biol Chem*. 2004;279(4):2632–2639.
17. Hu B, Wu Z, Phan SH. Smad3 mediates transforming growth factor-beta-induced alpha-smooth muscle actin expression. *Am J Respir Cell Mol Biol*. 2003;29(3 Pt 1):397–404.
18. Peinado H, Quintanilla M, Cano A. Transforming growth factor beta-1 induces snail transcription factor in epithelial cell lines: mechanisms for epithelial mesenchymal transitions. *J Biol Chem*. 2003;278(23):21113–21123.
19. Xu J, Lamouille S, Derynck R. TGF-beta-induced epithelial to mesenchymal transition. *Cell Res*. 2009;19(2):156–172.
20. Budi EH, Duan D, Derynck R. Transforming growth factor-β receptors and smads: regulatory complexity and functional versatility. *Trends Cell Biol*. 2017;27(9):658–672.
21. Feng XH, Derynck R. Specificity and versatility in tgf-beta signaling through Smads. *Annu Rev Cell Dev Biol*. 2005;21:659–693.

22. Yang X, Letterio JJ, Lechleider RJ, et al. Targeted disruption of SMAD3 results in impaired mucosal immunity and diminished T cell responsiveness to TGF-beta. *EMBO J*. 1999;18(5):1280—1291.
23. Roberts AB, Tian F, Byfield SD, et al. Smad3 is key to TGF-beta-mediated epithelial-to-mesenchymal transition, fibrosis, tumor suppression and metastasis. *Cytokine Growth Factor Rev*. 2006;17(1—2):19—27.
24. Jiang L, Kwong DL, Li Y, et al. HBP21, a chaperone of heat shock protein 70, functions as a tumor suppressor in hepatocellular carcinoma. *Carcinogenesis*. 2015;36(10):1111—1120.
25. Xie Y, Lv X, Ni D, et al. HPD degradation regulated by the TTC36-STK33-PELI1 signaling axis induces tyrosinemia and neurological damage. *Nat Commun*. 2019;10(1):4266.
26. Zhou Y, He Q, Chen J, et al. The expression patterns of Tetratricopeptide repeat domain 36 (Ttc36). *Gene Expr Patterns*. 2016;22(2):37—45.
27. Liu Y, Lv X, Tan R, et al. A modified TALEN-based strategy for rapidly and efficiently generating knockout mice for kidney development studies. *PLoS One*. 2014;9(1):e84893.
28. Huang KT, Wu CT, Huang KH, et al. Titanium nanoparticle inhalation induces renal fibrosis in mice via an oxidative stress upregulated transforming growth factor-β pathway. *Chem Res Toxicol*. 2015;28(3):354—364.
29. Gomis RR, Alarcón C, Nadal C, Van Poznak C, Massagué J. C/EBPβ at the core of the TGFbeta cytostatic response and its evasion in metastatic breast cancer cells. *Canc Cell*. 2006;10(3):203—214.
30. Zeisberg M, Maeshima Y, Mosterman B, Kalluri R. Renal fibrosis. Extracellular matrix microenvironment regulates migratory behavior of activated tubular epithelial cells. *Am J Pathol*. 2002;160(6):2001—2008.
31. Iwano M, Plieth D, Danoff TM, Xue C, Okada H, Neilson EG. Evidence that fibroblasts derive from epithelium during tissue fibrosis. *J Clin Invest*. 2002;110(3):341—350.
32. Yang J, Dai C, Liu Y. Hepatocyte growth factor gene therapy and angiotensin II blockade synergistically attenuate renal interstitial fibrosis in mice. *J Am Soc Nephrol*. 2002;13(10):2464—2477.
33. Sato M, Muragaki Y, Saika S, Roberts AB, Ooshima A. Targeted disruption of TGF-beta1/Smad3 signaling protects against renal tubulointerstitial fibrosis induced by unilateral ureteral obstruction. *J Clin Invest*. 2003;112(10):1486—1494.
34. Meng XM, Huang XR, Chung AC, et al. Smad2 protects against TGF-beta/Smad3-mediated renal fibrosis. *J Am Soc Nephrol*. 2010;21(9):1477—1487.
35. Fukuchi M, Imamura T, Chiba T, et al. Ligand-dependent degradation of Smad3 by a ubiquitin ligase complex of ROC1 and associated proteins. *Mol Biol Cell*. 2001;12(5):1431—1443.
36. Pless O, Kowenz-Leutz E, Knoblich M, et al. G9a-mediated lysine methylation alters the function of CCAAT/enhancer-binding protein-beta. *J Biol Chem*. 2008;283(39):26357—26363.
37. Roy SK, Hu J, Meng Q, et al. MEKK1 plays a critical role in activating the transcription factor C/EBP-beta-dependent gene expression in response to IFN-gamma. *Proc Natl Acad Sci U S A*. 2002;99(12):7945—7950.
38. Nieto MA. The snail superfamily of zinc-finger transcription factors. *Nat Rev Mol Cell Biol*. 2002;3(3):155—166.
39. Cano A, Pérez-Moreno MA, Rodrigo I, et al. The transcription factor snail controls epithelial-mesenchymal transitions by repressing E-cadherin expression. *Nat Cell Biol*. 2000;2(2):76—83.
40. Carver EA, Jiang R, Lan Y, Oram KF, Gridley T. The mouse snail gene encodes a key regulator of the epithelial-mesenchymal transition. *Mol Cell Biol*. 2001;21(23):8184—8188.
41. Grande MT, Sánchez-Laorden B, López-Blau C, et al. Erratum: snail1-induced partial epithelial-to-mesenchymal transition drives renal fibrosis in mice and can be targeted to reverse established disease. *Nat Med*. 2016;22(2):217.